PHYSICAL REVIEW A VOLUME 39, NUMBER 11 JUNE 1, 1989

Spectral geometry of power-law potentials in quantum mechanics

Richard L. Hall
Department of Mathematics, Concordia University, 1455 de Maisonneuve Boulevard West,
Montreal, Quebec, Canada H3G 1M8

(Received 8 December 1988)

It is supposed that a single particle moves in $\mathbb{R}^3$ in an attractive central power-law potential $V^{(q)}(r)=\text{sgn}(q)r^q$, $q>-2$, and obeys nonrelativistic quantum mechanics. This paper is concerned with the question: How do the discrete eigenvalues $E_{nl}(q)$ of the Hamiltonian $H=-\Delta+V^{(q)}$ depend on the power parameter q? Pure power-law potentials have the elementary property that, for $p<q$, $V^{(q)}(r)$ is a convex transformation of $V^{(p)}(r)$. This simple fact makes it possible to use "kinetic potentials" to construct a global geometrical theory for the spectrum of H and also for more general operators of the form $H'=-\Delta+\sum_q A^{(q)}V^{(q)}$, $A^{(q)}\in\mathbb{R}$. This geometrical approach greatly simplifies the description of the spectra and also facilitates the construction of some general eigenvalue bounds and approximation formulas.

I. INTRODUCTION

This article is concerned principally with the following simple question: If a particle moves in a pure attractive power-law potential $V(r)=\text{sgn}(q)r^q$, how do the Schrödinger eigenvalues depend on the power parameter q? Here the sign factor $\text{sgn}(q)$ is included to guarantee that the potential is attractive when $q<0$, that is to say, so that $V'(r)>0$.

After over 60 years of quantum mechanics the hydrogenic atom $q=-1$ and the harmonic oscillator $q=2$ may perhaps be described as the most important two examples of physical systems which are well understood in terms of the theory. Although the discrete energy spectra are very different, we usually group these problems together because of their physical importance for atomic and molecular physics, and because they are soluble. In this paper we shall use geometrical methods to recast these problems in such a way that the spectra appear very similar. Since our approach is global with respect to the power parameter $q>-2$, we capture at the same time the discrete spectra of other problems such as the linear potential $q=1$, which has recently become important for the construction of models for systems composed of quarks.

Fortuitously, the representation for the discrete spectra introduced by our geometrical theory allows us to treat not only pure powers but also arbitrary linear combinations. This means that important physical problems involving, for example, anharmonic oscillators or the linear-plus-Coulomb potential can also be accommodated. Meanwhile, by exploiting the exactly soluble problems $q=1$ and $q=2$, we are able to construct convenient global-approximation formulas for this whole range of interesting physical problems.

We consider now a single particle which moves in three spatial dimensions, is bound by an attractive central power-law potential, and obeys nonrelativistic quantum mechanics. If units are chosen so that $\hbar=1$ and $m=\frac{1}{2}$, then such a system will have the Hamiltonian $H^{(v)}$ given by

$$H^{(v)}=-\Delta+v\,\text{sgn}(q)r^q,\quad q>-2,\quad q\neq 0\,, \tag{1.1}$$

where $r=|\vec{r}|$ and $v>0$ is a constant coupling parameter. For most physical situations the restriction $q\geq -1$ is appropriate, but from a mathematical point of view[1-3] we can allow $q>-2$. In this paper we shall study the dependence of the discrete spectrum $E_{nl}^{(v)}(q)$ of $H^{(v)}$ on the power parameter q. Here, $l=0,1,2,3,\ldots$, is the usual angular momentum quantum number, and $n=1,2,3,\ldots$, is a radial quantum number which enumerates the discrete eigenvalues in each angular momentum subspace; that is to say, $E_{nl}^{(v)}(q)\leq E_{ml}^{(v)}(q)$, $n<m$. For $q>-2$ and $q\neq 0$, all these discrete eigenvalues exist. With our labeling convention, the eigenvalue $E_{nl}^{(v)}(q)$ always has degeneracy of *precisely* $2l+1$.

We can determine the dependence of the eigenvalues on the coupling parameter v by the use of elementary scaling arguments. Once we have dealt with this aspect of the spectrum we shall be able to simplify our notation and concentration on the dependence of the spectrum on q alone. If we replace r or σr, where $\sigma>0$ is a scaling constant, then the Hamiltonian has the form

$$H^{(v)}=-\sigma^{-2}\Delta+v\sigma^{q}\text{sgn}(q)r^q\,.$$

Consequently, by choosing the scale σ so that $v\sigma^{q+2}=1$, we see that $\sigma^2H^{(v)}=H^{(1)}$ and therefore the eigenvalues of $H^{(v)}$ are $\sigma^{-2}=v^{2/(q+2)}$ times the eigenvalues of $H^{(1)}$. Thus, in terms of our (still uncomfortable) notation, we find

$$E_{nl}^{(v)}(q)=v^{2/(q+2)}E_{nl}^{(1)}(q)=F_{nl}^{(q)}(v)\,. \tag{1.2}$$

The function $F_{nl}^{(q)}(v)$ is called an *energy trajectory* and tells us how the eigenvalue depends on the coupling constant; this functional dependence will be important later. Since (1.2) completely solves the problem of the dependence on v, it is convenient to simplify our notation by defining the Hamiltonian $H = H^{(1)}$ and the corresponding spectral functions $E_{nl}(q) = E_{nl}^{(1)}(q)$. Thus we have

$$H = -\Delta + \text{sgn}(q) r^q, \quad q > -2, \quad q \neq 0 \ . \tag{1.3}$$

If we set $q = 0$ in (1.3), the corresponding Hamiltonian H has no discrete eigenvalues. However, the bottoms of the spectra of the shifted kinetic energy operators $-\Delta \pm 1$ are, respectively, ± 1, and the eigenvalues $E_{nl}(q)$ all approach (one of) these limits as q approaches zero, respectively, from positive or negative values. It is therefore convenient to define the value of $|E_{nl}(q)|$ for $q = 0$ to be 1. The principal goal of this article then is to study the family of continuous functions of q given by $|E_{nl}(q)|$. We shall sometimes omit the labels nl when our arguments apply equally well to any particular representative of this class of functions of q.

We are fortunate in having some exactly soluble special cases at our disposal. For the well-known hydrogenic atom $q = -1$ and the harmonic oscillator $q = 2$ we have the formulas

$$E_{nl}(-1) = -[2(n+l)]^{-2} \tag{1.4}$$

and

$$E_{nl}(2) = 4n + 2l - 1 \ . \tag{1.5}$$

To these we may add the linear potential which, for S states, is exactly soluble[4] in terms of the zeros (z_n) of Airy's function $\text{Ai}(r)$. We have

$$E_{n0}(1) = -z_n, \quad \text{Ai}(z_n) = 0, \quad n = 1,2,3,\ldots \ . \tag{1.6}$$

In Fig. 1 we exhibit graphs of the functions $|E_{n0}(q)|$ for $n = 1,2,3,4,5,6$. Since, as $q \to \infty$, the potential approaches an infinite square well with width 1, we know that $\lim_{q \to \infty} |E_{n0}(q)| = (n\pi)^2$. Near $q = 0$ the figure must be interpreted with care, since, as we shall see in Sec. III, the graphs actually have infinite slopes at that point. This is not a numerical problem, for the eigenvalues near $q = 0$ are very easy to find numerically with high accuracy. The difficulty arises because of the extremely slow approach to infinite slope as q approaches zero. An elementary function which behaves[5] like this is $y = |x|^{1/x}$, with the assigned value of 1 at $x = 0$; for this function, $y'(x)$ is unbounded as $x \to 0$, but even when $x = 10^{-10}$ we reach only the value $y'(x) \approx -22.03$. Such pathology is, of course, usually invisible on a graph drawn with the aid of a computer. One of our goals is to find a representation for $|E_{nl}(q)|$ which is smoother and less complicated, and therefore easier to approximate. We base our work on a nonperturbative geometrical theory which describes how the spectrum of H is altered under a smooth transformation of the potential.

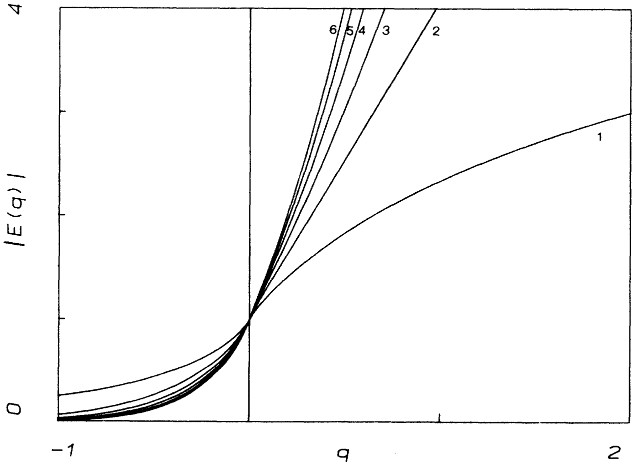

FIG. 1. Graphs of the absolute eigenvalues $|E_{nl}(q)|$ for $l = 0$ and $n = 1,2,3,4,5,6$. There are no discrete eigenvalues for $q = 0$ but, in order to make them continuous, the graphs are all assigned here the value zero. The curves cross over at $q = 0$ and they have infinite slopes at that point.

In Sec. II, we outline the theory of *kinetic potentials*.[6,7] With the aid of this geometrical theory we are able in Sec. III to analyze the family of power-law potentials in terms of one another. For example, a harmonic-oscillator potential may be viewed as the envelope curve of a family of hydrogenic potentials. If such an envelope representation is constructed locally, for every power-law potential, then the functions $P_{nl}(q)$ given by

$$P_{nl}(q) = \left[\frac{|E_{nl}(q)|}{\eta(q)} \right]^{(2+q)/2q}, \quad q > -1, \quad q \neq 0 \tag{1.7}$$

where

$$\eta(q) = \left[\frac{q}{2} + 1 \right] \left| \frac{2}{q} \right|^{q/(q+2)}, \quad q \neq 0, \quad \eta(0) = 1 \ , \tag{1.8}$$

emerge naturally from the theory and we can prove that these functions are monotonically increasing functions of q. The limiting values $\lim_{q \to 0}[P_{nl}(q)]$ are finite and we assign $P_{nl}(0)$, respectively, to these limits in order to make the P functions continuous.

Graphs of $P_{n0}(q)$ for $n = 1,2,3,4,5,6$ are shown in Fig. 2. The slope pathology in the corresponding graphs of $|E_{nl}(q)|$ has now been factored out by $\eta(q)$ and the new graphs do not cross over each other at $q = 0$. Moreover, although $|E_{nl}(0)|/g(0) = 1$, the values $P_{nl}(0)$ vary with n and l so that the degenerate collapse at $q = 0$ of all the eigenvalue curves to the value 1 has been removed by the transformation.

For example, in terms of the representation $P_{nl}(q)$, the familiar but very different hydrogenic and harmonic-oscillator discrete spectra now look remarkably similar. More specifically, we have from (1.4), (1.5), and (1.7)

$$P_{nl}(-1) = n + l \tag{1.9}$$

and

$$P_{nl}(2) = 2n + l - \tfrac{1}{2} \ . \tag{1.10}$$

Thus, with any fixed value of n, the ratio $P_{nl}(-1)/P_{nl}(2)$ tends to the limit 1 as l increases to infinity. These analytical results and the representation (1.7) pave the way for the construction of various approximate eigenvalue formulas for pure power laws in Sec. IV, and for general linear combinations in Sec. V. In Sec. VI we study the Coulomb-plus-square-root example with Ham-

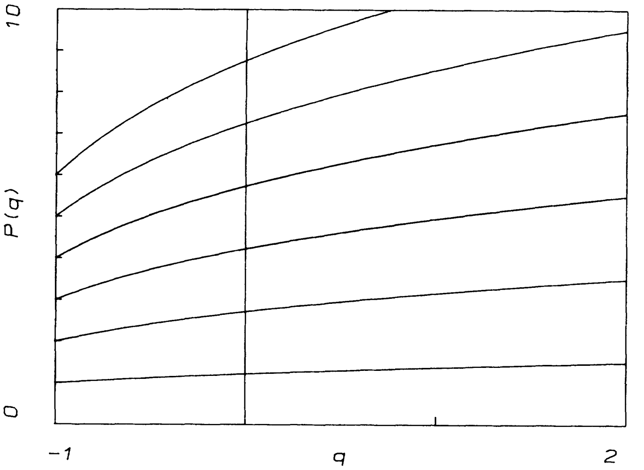

FIG. 2. The same six eigenvalues as shown in Fig. 1 are now plotted in the representation $P_{nl}(q)$ defined by Eq. (1.7). The new curves are smooth, and, at $q=0$, are separated, one from another, and they do not cross over.

iltonian given by $H=-\Delta-1/r+\lambda r^{1/2}$ and compare our results to accurate data computed numerically.

II. KINETIC POTENTIALS

We consider the spectrum of a Schrödinger operator H given by

$$H=-\Delta+vf(r)\ , \tag{2.1}$$

where v is a positive coupling constant. The attractive central potential shape $f(r)$ has one of the two forms

$$f(r)=g(h(r))\ , \tag{2.2}$$

or

$$f(r)=f^{(1)}(r)+f^{(2)}(r)\ , \tag{2.3}$$

where g is a smooth increasing transformation of the attractive central potential $h(r)$. Suppose that the spectra are known for each of the Hamiltonians H in which the potential $f(r)$ equals one of the component potentials: What can be said about the spectra of the corresponding Hamiltonians in which the potentials $f(r)$ are given either by smooth transformations or by sums, as in (2.2) or (2.3)? *Kinetic potentials*[6] were introduced to treat this question and to provide a global approximation theory for the spectra. We shall outline here a sufficient amount of the theory to provide us with the formulas required by the present application to power-law potentials, and we refer the reader to Ref. 6 for more details. We shall begin with a discussion of the ground-state energies and extend the results to the excited states afterwards.

From the point of view of functional analysis[1-3] one regards the Hamiltonian operator H as a perturbation of the Laplacian $-\Delta$. Kinetic potentials are derived from the following analytical realization of this point of view. We first fix $\langle -\Delta \rangle = s > 0$; this defines a certain subset $\mathcal{D}_s$ of the domain $\mathcal{D}(H)$ of H. We then minimize $\langle f(r) \rangle$ over $\mathcal{D}_s$, and the result, as a function of the "mean" kinetic energy s, is called the (ground-state) *kinetic potential* $\bar{f}_{10}(s)$ associated with the potential shape $f(r)$; this name is a contraction of the more explanatory term *minimum mean isokinetic potential.* Thus for the ground state we have

$$\bar{f}_{10}(s)=\inf_{\substack{\psi\in\mathcal{D}(H)\\ \|\psi\|=1\\ (\psi,-\Delta\psi)=s}}(\psi,f\psi)\ . \tag{2.4}$$

We notice that only the potential *shape* $f(r)$ is employed in the definition of the corresponding kinetic potential $\bar{f}(s)$; the coupling parameter v is not involved. It is as though we had only done that part of the min-max procedure which has to do with *shape*; at this stage, the strength has not yet been fully taken into account. The ground-state energy is then recovered from the kinetic potential by a final stage of minimization given, in general, by

$$E_{nl}=F_{nl}(v)=\min_{s>0}\,[s+v\bar{f}_{nl}(s)]\ . \tag{2.5}$$

Thus, instead of going directly from the potential shape $f(r)$ to the energy trajectory $E_{nl}=F_{nl}(v)$, we first find, corresponding to each eigenvalue, an intermediate form, the kinetic potential $\bar{f}_{nl}(s)$. We shall define these "higher" kinetic potentials below. The advantage of using kinetic potentials is that they have some very useful transformation and composition properties. The results we shall need here can be summarized by the following equations. Under scaling and shifts we have

$$f(r)=A+Bh(r/a)\rightarrow\bar{f}_{nl}(s)=A+B\bar{h}_{nl}(sa^2),\quad a,B>0\ . \tag{2.6}$$

From the variational characterization of the spectra it is straightforward to show that the potentials, the kinetic potentials, and the spectra are ordered in the same fashion:

$$f^{(1)}(r)<f^{(2)}(r)\rightarrow\bar{f}_{nl}^{(1)}(s)\le\bar{f}_{nl}^{(2)}(s)\rightarrow F_{nl}^{(1)}(v)\le F_{nl}^{(2)}(v)\ . \tag{2.7}$$

Under smooth (increasing) transformations we have

$$f(r)=g(h(r))\rightarrow\begin{cases}\bar{f}_{nl}(s)\le g(\bar{h}_{nl}(s))\\ \bar{f}_{nl}(s)\ge g(\bar{h}_{nl}(s))\end{cases}, \tag{2.8}$$

where we get a lower bound ($\ge$) if g is convex, and an upper bound ($\le$) if g is concave; if the convexity of g is not zero, then the inequalities in (2.8) are strict ($<$ or $>$).

The next result, which, in general, we call the "sum approximation," provides a lower bound for the *bottom* of each angular momentum subspace. We have

$$f(r)=f^{(1)}(r)+f^{(2)}(r)\rightarrow\bar{f}_{nl}(s)\approx\bar{f}_{nl}^{(1)}(s)+\bar{f}_{nl}^{(2)}(s)\ , \tag{2.9}$$

and for $n=1$, $\bar{f}_{1l}(s)\ge\bar{f}_{1l}^{(1)}(s)+\bar{f}_{1l}^{(2)}(s)$. The sum approximation (2.9) is very good because it turns out that, unlike the spectra, the kinetic potentials are "almost additive." That is to say, although the spectrum corresponding to the sum of two potentials is, in general, not at all close to the sum of the two individual spectra, the situation is very different at the "intermediate stage" the kinetic potential stage, of the min-max procedure; the kinetic potential corresponding to the sum of two potentials is to a good approximation just the sum of the component kinetic potentials.

The final result concerns only the ground state estimated by a trial function with shape g and minimized with respect to scale; here the "trial" kinetic potentials are exactly additive and the result yields, of course, an upper energy bound,

$$f^{(1)}(r)+f^{(2)}(r)\rightarrow \bar{f}_{10}(s)\le \bar{f}_g(s)=\bar{f}_g^{(1)}(s)+\bar{f}_g^{(2)}(s) \ . \tag{2.10}$$

The abstract definition (2.4) of kinetic potentials (or its generalization, given below) is *not* used for finding the component kinetic potentials. Instead, one inverts the Legendre transformation (2.5) to obtain $\bar{f}_{nl}(s)$ in terms of the known energy trajectory $E_{nl}=F_{nl}(v)$. Thus from (2.5) we can immediately derive the following general parametric form for $\bar{f}_{nl}(s)$ in terms of the trajectory function $F_{nl}(v)$. We obtain

$$s=F_{nl}(v)-vF'_{nl}(v), \quad \bar{f}_{nl}(s)=F'_{nl}(v) \ . \tag{2.11}$$

The simplicity of (2.11) is important because the abstract definition of the higher kinetic potentials would seem to present some difficulty if we wished to use it directly. For completeness and clarity we now outline the general definition of these objects. We suppose that D_{nl} is an n-dimensional subspace of the intersection of the domain $\mathcal{D}(H)$ and the angular momentum subspace of $L^2(R^3)$ labeled by the spherical harmonic $Y_l^m(\theta,\phi)$ with, say, $m=0$. We now consider the union $\mathcal{D}_{nl}$ of all σ-scaled transformations $\sigma\in R^+$ of D_{nl}, in which each wave function $\psi(\vec{r})$ in D_{nl} is replaced by use of the rule $\psi(\vec{r})\rightarrow\psi(\vec{r}/\sigma)$. This large union of subspaces is itself no longer a subspace; however, because $\mathcal{D}_{nl}$ contains all possible scales, we can always satisfy the constraint $(\psi,-\Delta\psi)=s$ for some $\psi\in D_{nl}\subset\mathcal{D}_{nl}$. The idea here is that one first chooses the n-dimensional space D_{nl} and then generates the larger union $\mathcal{D}_{nl}$ of all "scaled" versions of D_{nl}. The general definition of $\bar{f}_{nl}(s)$ is then as follows:

$$\bar{f}_{nl}(s)=\inf_{D_{nl}} \sup_{\substack{\psi\in\mathcal{D}_{nl}\\ \|\psi\|=1\\ (\psi,-\Delta\psi)=s}} (\psi,f\psi) \ . \tag{2.12}$$

Fortunately, because of (2.11), we shall not have to work with (2.12) directly in this paper.

In the case of the power-law potentials

$$f^{(q)}(r)=\mathrm{sgn}(q)r^q \ , \tag{2.13}$$

we obtain from (1.2) and (2.11)

$$\bar{f}_{nl}{}^{(q)}(s)=(2/q)|qE_{nl}(q)/(2+q)|^{(q+2)/2}s^{-q/2} \ , \tag{2.14}$$

where $E_{nl}(q)$ is the n,l eigenvalue of $H=-\Delta+\mathrm{sgn}(q)r^q$. From the exact eigenvalues (1.4) and (1.5), we have, therefore, the following exact kinetic potentials:

$$f(r)=-r^{-1}\rightarrow \bar{f}_{nl}(s)=-s^{1/2}/(n+l) \tag{2.15}$$

and

$$f(r)=r^2\rightarrow \bar{f}_{nl}(s)=s^{-1}(2n+l-\tfrac{1}{2})^2 \ . \tag{2.16}$$

The approximate kinetic potentials corresponding to sums and smooth transformations of pure power-law potentials can now be constructed by means of Eqs. (2.6)–(2.9), and the corresponding approximate energy trajectories for the composite potential are given by simply inverting (2.11), or, equivalently, rewriting (2.5), that is to say, from the equations

$$E_{nl}=F_{nl}(v)=s+v\bar{f}_{nl}(s), \quad v^{-1}=-\bar{f}'_{nl}(s) \ , \tag{2.17}$$

which are, of course, simply the parametric equations for the energy trajectory $(v,F_{nl}(v))$ since v and $F_{nl}(v)$ are each given as functions of the curve parameter s.

We are therefore immediately able to treat a potential with shape given by the general linear combination

$$f(r)=\sum_q A^{(q)}\mathrm{sgn}(q)r^q, \quad q>-2, \quad A^{(q)}\ge 0 \ . \tag{2.18}$$

Since we also have an overall coupling constant v in our formulation, we obviously have one too many coupling parameters. However, it is convenient to make the necessary choice of which parameter to eliminate during the course of an application. If we now use the more convenient parameter $t=s^{-1/2}$, we find from (2.9) and (2.14) the following *approximate* parametric equations for the energy trajectories corresponding to the general linear combination of powers given in (2.18):

$$\begin{aligned} F_{nl}(v)&=t^{-2}+v\sum_q A^{(q)}\left|\frac{qE_{nl}(q)}{2+q}\right|^{(q+2)/2}\frac{2t^q}{q} \ , \\ v^{-1}&=\sum_q A^{(q)}\left|\frac{qt^2E_{nl}(q)}{2+q}\right|^{(q+2)/2} \ . \end{aligned} \tag{2.19}$$

Generalizations of these results to include other types of potential "components," such as the log and Hulthén potentials, may be found in Refs. 6 and 7. With certain notable exceptions, such as $q=-1$ and $q=2$, the missing elements in this very general scheme are the pure power-law eigenvalues $E_{nl}(q)$. It is the main purpose of this paper to use our geometrical theory to supply approximations for these eigenvalues.

III. THE SPECTRAL GEOMETRY OF POWER-LAW POTENTIALS

The principal results of this section are a consequence of the simple geometrical fact that if we write one power potential as a function g of another, then g is either convex or concave. Thus we have

$$\mathrm{sgn}(p)r^p=g(\mathrm{sgn}(q)r^q)=g(h), \quad pq\neq 0 \ , \tag{3.1}$$

where, for each fixed p and q, $p\neq q$, we have

$$g(h)=\mathrm{sgn}(p)(h\ \mathrm{sgn}(q))^{p/q} \tag{3.2}$$

and $h\ \mathrm{sgn}(q)=r^q\geq 0$. Consequently, we find

$$g'(h)=\left|\frac{p}{q}\right|(h\ \mathrm{sgn}(q))^{p/q-1}\geq 0 \tag{3.3}$$

and

$$g''(h)=\frac{|p|}{q^2}(p-q)(h\ \mathrm{sgn}(q))^{p/q-2}\ . \tag{3.4}$$

Hence, the function g is convex if $p>q$ and concave if $p<q$.

Having established definite convexity properties for the transformation function g, we can now exploit the variational implications by using kinetic potentials. Let us suppose, for definiteness, that $pq\neq 0$ and $p>q$, so that g is *strictly convex*. We then have from (2.8)

$$\bar{f}_{nl}{}^{(p)}(s)<g(\bar{f}_{nl}{}^{(q)}(s)),\quad p>q\ . \tag{3.5}$$

If we now substitute the explicit forms for the kinetic potentials (2.14) into (3.5) and cancel the nonzero factor $s^{-p/2}$ from both sides, we obtain

$$(2/p)|pE_{nl}(p)/(2+p)|^{(p+2)/2} > \mathrm{sgn}(p)\left\{\left|\frac{2}{q}\right||qE_{nl}(q)/(2+q)|^{(q+2)/2}\right\}^{p/q}\ . \tag{3.6}$$

We now apply a sequence of two algebraic operations to both sides of (3.6). We first multiply by $\mathrm{sgn}(p)$, and then we take the $1/p$ power. In the case that $p>0$, both of these operations leave the inequality in (3.5) unchanged; in the case that $p<0$, the inequality is reversed twice. Hence in both cases we conclude

$$P_{nl}(p)>P_{nl}(q),\quad pq\neq 0,\quad p>q\geq -1\ , \tag{3.7}$$

where, as in Sec. I,

$$P_{nl}(q)=\left[\frac{|E_{nl}(q)|}{\eta(q)}\right]^{(2+q)/2q} \tag{3.8}$$

and

$$\eta(q)=\left[\frac{q}{2}+1\right]\left|\frac{2}{q}\right|^{q/(q+2)},\quad q\neq 0,\quad \eta(0)=1\ . \tag{3.9}$$

Thus, with the aid of the variational properties of Schrödinger eigenvalues, we have generated the curious functions $P_{nl}(q)$ and we have been able to prove that they are monotonically increasing functions of q. These functions capture the variation of the eigenvalues $E_{nl}(q)$ with q in a particularly simple form. We already exhibited some graphs of $P_{n0}(q)$ in Fig. 2 of Sec. I. In Fig. 3 here we show graphs of $P_{nl}(q)$ for all $\{n,l\}$, such that $n+l\leq 6$. These graphs show clearly how the degeneracy of the hydrogen atom $(q=1)$ transforms smoothly into the degeneracy of the harmonic oscillator $(q=2)$ as the power q increases from -1 to 2. The corresponding graphs of $E_{nl}(q)$ are much more complicated.

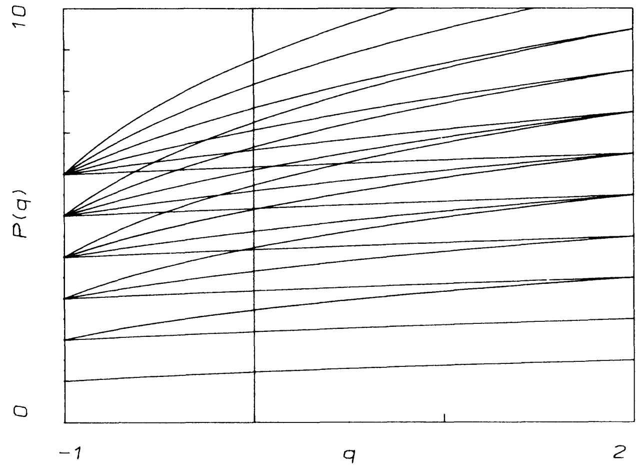

FIG. 3. Graphs of $P_{nl}(q)$ for all $\{n,l\}$, such that $n+l\leq 6$. These graphs show clearly how the degeneracy of the hydrogen atom $(q=-1)$ transforms smoothly into the degeneracy of the harmonic oscillator $(q=2)$ as the power q is increased from -1 to 2. It is proved in Sec. IV that these graphs are monotonically increasing for all $q>-2$; we conjecture that they are also concave. The corresponding graphs of $E_{nl}(q)$ are much more complicated.

By using logarithms in (3.8) and taking the formal limit (that is to say, the unproven limit) as $q\to 0$, we find the following expression which we use as a "working" definition of $P_{nl}(0)$:

$$P_{nl}(0)=\lim_{q\to 0}[P_{nl}(q)]=\frac{d}{dq}[|E_{nl}(q)|/\eta(q)]\bigg|_{q=0}\ . \tag{3.10}$$

It is perhaps intuitively clear that the wild behavior of $E_{nl}(q)$ near $q=0$ has indeed been factored away by $\eta(q)$, and our graphs are consistent with this since $\eta(q)$ alone does indeed have an infinite slope at $q=0$, whereas (numerically) the $P_{nl}(q)$ do not. Some more analytical effort would have to be brought to bear on the Hamiltonian operator in order to make (3.10) mathematically secure. However, since we have no intention of relying on this expression in any technical way, we shall rest the matter with (3.10) which indicates from the mathematical viewpoint how it could be that, although the $E_{nl}(q)$ curves all cross over at $q=0$, the corresponding $P_{nl}(q)$ curves shown in Fig. 3 are distinct there.

IV. APPROXIMATIONS FOR PURE POWERS

Any approximation we obtain for the slowly varying functions $P_{nl}(q)$ leads in turn to an approximation for $E_{nl}(q)$. For example, our main result, the monotonicity of $P_{nl}(q)$, along with the specific values (1.9) and (1.10), immediately yield the following inequalities:

$$n+l\leq P_{nl}(q)\leq 2n+l-\tfrac{1}{2},\quad -1\leq q\leq 2\ . \tag{4.1}$$

It is perhaps remarkable that, in this picture, the spectra of the hydrogenic atom and the harmonic oscillator appear very similar. However, in order to obtain numerically useful results we must now devise a suitable interpolation over some range of q values.

In this endeavor we are guided by the fact that all these eigenvalues are in any case very easy to find today by direct numerical methods. Consequently, although our formulation is theoretically interesting, the only immediate practical outcome would be a *simple* formula, something which is easy to use for exploration.

We have performed what have come to be called "computer experiments," and on the basis of these investigations and the philosophy outlined above we have arrived at the following conclusions. Firstly, although we are still far from a theoretical proof, it is clear experimentally that the curves $P_{nl}(q)$ are *concave* functions of q [that is to say, $P''_{nl}(q)<0$]. If this result could be *proved* mathematically; then, by the use of tangents and chords to the graph of $P_{nl}(q)$ we should immediately obtain a large variety of new eigenvalue *bounds*; however, we do not have a proof. We also found that for the interval $q\in[-1,2]$ the graphs of the functions $[P_{nl}(q)]^{\alpha}$, in which α is a constant, become approximately straight when α is between 3 and 4. We therefore choose a value for the parameter α so that the linear interpolation of $[P_{nl}(q)]^{\alpha}$ gives the exact result for the ground state of the linear potential, that is to say, for $P_{10}(1)$. Therefore, from (3.8), we see that this linear-interpolation approximation is given by the formula

$$P_{nl}^{A}(q)=\left\{[P_{nl}(-1)]^{\alpha}+\frac{(q+1)}{3}\{[P_{nl}(2)]^{\alpha}-[P_{nl}(-1)]^{\alpha}\}\right\}^{1/\alpha}$$
$$=\left\{(n+l)^{\alpha}+\frac{(q+1)}{3}[(2n+l-\tfrac{1}{2})^{\alpha}-(n+l)^{\alpha}]\right\}^{1/\alpha} . \tag{4.2}$$

Hence the equation we must solve for the parameter α is given by

$$\{1+\tfrac{2}{3}[(\tfrac{3}{2})^{\alpha}-1]\}^{1/\alpha}=\left[\frac{E_{10}(1)}{(3/2)2^{1/3}}\right]^{3/2} , \tag{4.3}$$

where, from (1.6), $E_{10}(1)\approx 2.338\,108$. By solving (4.3) numerically we find

$$\alpha\approx 3.239\,692 . \tag{4.4}$$

This value of α completes the specification of the approximation (4.2). The approximate energies $E_{nl}^{A}(q)$ are, of course, obtained from $P_{nl}^{A}(q)$ by inverting the definition (3.8), that is to say, from

$$E_{nl}^{A}(q)=\text{sgn}(q)\left[\frac{q}{2}+1\right]\left|\frac{2}{q}\right|^{q/(q+2)}[P_{nl}^{A}(q)]^{2q/(q+2)} . \tag{4.5}$$

Such formulas fit comfortably in the memory of a pocket calculator.

It is of course interesting to compare the approximation defined by (4.2), (4.4), and (4.5), with some accurate eigenvalues found numerically. We do this in the Table I,

TABLE I. Some eigenvalues $E_{nl}(q)$ and their corresponding approximations $E_{nl}^{A}(q)$ given by Eq. (4.5). The percentage errors decrease with increasing l, and they increase with n and with the distance from the special q values $q=-1$ and 2.

E_{nl}	$q=-0.5$	$q=0.5$	$q=1$	$q=1.5$	$q=2.5$
E_{10}	-0.4380	1.8334	2.3381	2.7081	3.2422
E_{10}^{A}	-0.4375	1.8338	2.3381	2.7076	3.2443
E_{20}	-0.2632	2.5506	4.0880	5.5857	8.3133
E_{20}^{A}	-0.2621	2.5462	4.0730	5.5676	8.3620
E_{50}	-0.1386	3.7934	7.9441	13.142	25.205
E_{50}^{A}	-0.1378	3.7806	7.8965	13.077	25.409
E_{11}	-0.2866	2.3005	3.3613	4.2508	5.6389
E_{11}^{A}	-0.2878	2.2937	3.3489	4.2400	5.6592
E_{21}	-0.2098	2.8543	4.8844	6.9660	10.938
E_{21}^{A}	-0.2103	2.8458	4.8634	6.9430	10.997
E_{51}	-0.1264	3.9627	8.5152	14.337	28.144
E_{51}^{A}	-0.1260	3.9513	8.4723	14.277	28.343
E_{15}	-0.1413	3.4424	6.4930	9.7662	16.067
E_{15}^{A}	-0.1417	3.4355	6.4759	9.7478	16.112
E_{25}	-0.1249	3.7704	7.6370	12.171	21.884
E_{25}^{A}	-0.1256	3.7569	7.6020	12.132	21.988
E_{55}	$-0.094\,78$	4.5743	10.692	19.028	40.055
E_{55}^{A}	$-0.095\,14$	4.5580	10.640	18.958	40.289

which exhibits the eigenvalues $E_{nl}(q)$ and the corresponding approximations $E^{A}_{nl}(q)$ for n, $l \leq 5$, and $q=-0.5, 0.5, 1.0, 1.5, 2.5$. By construction, the formula gives the exact energy whenever $q=-1$ or 2, and also for the ground state with $q=1$. In this table the highest-percentage error is 0.81% for the case $E^{A}_{50}(2.5)$; the error is often much less. From the inequality (4.1) we know that, for any fixed n, the *percentage* error in the approximation decreases to zero as l is increased without bound.

V. GENERAL LINEAR COMBINATIONS OF POWERS

By serendipitous good fortune it turns out that the $P_{nl}(q)$ functions, which emerged naturally from our geometrical theory in Sec. III, greatly simplify the sum approximation (2.19). This is most convenient since it is actually the $P_{nl}(q)$ rather than the $E_{nl}(q)$ that we have been able to approximate.

If we substitute the $P_{nl}(q)$ from their definition (1.7) into (2.19) we obtain the following approximate parametric equations for the energy trajectory associated with the linear combination $f(r)=\sum_q A^{(q)}\text{sgn}(q)r^q$:

$$\begin{aligned} v^{-1}F_{nl}(v) &= \sum_q \text{sgn}(q)(1+1/q)A^{(q)}[tP_{nl}(q)]^q , \\ v^{-1} &= \sum_q \left|\frac{q}{2}\right| A^{(q)}[tP_{nl}(q)]^q t^2 . \end{aligned} \tag{5.1}$$

We recall that $F_{nl}(v)$ is the nl eigenvalue of the Hamiltonian $H=-\Delta+vf(r)$. We know[6] that, for the bottom of each angular momentum subspace (that is to say, $n=0$, for each l), this approximation is in fact a *lower*-energy bound. Furthermore, if the sum over q is from q_1 to q_2, then, by using, respectively, either $P_{nl}(q_1)$ for every occurrence of P in (5.1), or, alternatively, $P_{nl}(q_2)$ for every P, we obtain, respectively, lower and upper energy bounds which are valid for *all* n and l. This follows from (2.8) and the fact that every term in the potential sum is both a convex function of $\text{sgn}(q_1)r^{q_1}$ and a concave function of $\text{sgn}(q_2)r^{q_2}$. If we use the approximations $P^{A}_{nl}(q)$ given by (4.2) for the $P_{nl}(q)$, then we get a convenient approximation which is not, however, known to be an energy *bound*. What we have here is the generalization of the results which we have discussed earlier for linear-plus-Coulomb[7] potential and the quartic-anharmonic oscillator;[8] now the various energy bounds and the approximation apply to any linear combination of power-law components.

VI. THE POTENTIAL $f(r)=-1/r+\lambda r^{1/2}$

As an example with linear combinations we consider the Hamiltonian given by

$$\mathcal{H}=-\alpha\Delta-\beta/r+\gamma r^{1/2} , \tag{6.1}$$

where the coefficients α, β, and γ are all positive. If the eigenvalues of $\mathcal{H}$ are given by $\mathcal{E}=\mathcal{E}(\alpha,\beta,\gamma)$, then, by elementary scaling arguments, we can show that

$$\mathcal{E}(\alpha,\beta,\gamma)=\frac{\beta^2}{\alpha}\mathcal{E}(1,1,\lambda), \quad \lambda=\gamma(\alpha/\beta^3)^{1/2} . \tag{6.2}$$

In view of (6.2) we need only consider the simpler one-parameter Hamiltonian H given by

$$H=-\Delta-1/r+\lambda r^{1/2} . \tag{6.3}$$

If we apply the theory of Sec. V to this problem by setting $v=1$, $A^{(-1)}=1$, and $A^{(1/2)}=\lambda$ in (5.1), then we obtain the following parametric equations for E_{nl} as a function of the $r^{1/2}$ coupling λ:

$$\begin{aligned} E_{nl} &= -\tfrac{1}{2}[t(n+l)]^{-1}+\tfrac{5}{4}\lambda[tP^{A}_{nl}(1/2)]^{1/2} , \\ 1 &= \tfrac{1}{2}[t(n+l)]^{-1}+\tfrac{1}{4}\lambda[tP^{A}_{nl}(1/2)]^{1/2}t^2 , \end{aligned} \tag{6.4}$$

where the coefficients $P^{A}_{nl}(1/2)$ are provided by the general formula (4.2) with $q=\frac{1}{2}$. The results we obtain in this way are compared in Table II, with some accurate data found by direct numerical integration of Schrödinger's equation.

VII. CONCLUSION

The purpose of this paper has been to explore some geometrical aspects of the Schrödinger eigenvalue problem. Each potential shape $f(r)$ leads to a family of energy trajectories $F_{nl}(v)$ which describe how the eigenvalues depend on the coupling constant. If a transformation is applied to f, one would like to know how the trajectory

TABLE II. Some approximate eigenvalues E^{A}_{nl} given by Eq. (6.2) for the Hamiltonian $H=-\Delta-1/r+\lambda r^{1/2}$, along with accurate values computed numerically.

		$\lambda=0.01$		$\lambda=1$		$\lambda=100$	
n	l	Approx.	Num. Comp.	Approx.	Num. Comp.	Approx.	Num. Comp.
1	0	−0.2339	−0.2334	1.1107	1.1275	69.082	69.211
1	1	−0.0331	−0.0325	1.9282	1.9413	89.153	89.468
1	5	0.0613	0.0616	3.2945	3.3025	135.89	136.18
2	0	−0.0291	−0.0296	2.1626	2.1630	99.088	99.268
2	1	0.0172	0.0176	2.5827	2.5962	111.70	112.07
2	5	0.0725	0.0731	3.6310	3.6465	148.78	149.33
5	0	0.0628	0.0610	3.6026	3.5986	149.41	149.82
5	1	0.0726	0.0723	3.8003	3.8093	156.36	156.81
5	5	0.0983	0.0990	4.4615	4.4800	180.85	181.52

functions F are transformed. The approach we have used is geometrical and global and is complementary to the large amount of work which has been done in perturbation theory to study the effects of *small* changes to f.

In a curious self-referential fashion, we have analyzed the power-law potentials as convex or concave transformations of each other. By the application of kinetic potentials this led to a new representation $P_{nl}(q)$ for the eigenvalues of $H=-\Delta+\mathrm{sgn}(q)r^q$ which is smooth, momotonically increasing, and straightforward to approximate. On the basis of computer experiments, we conjecture that the P functions are *concave*. However, in spite of the interesting concavity results in Sec. 3.5 of the book by Thirring,[3] and also of the convexity results of our own concerning kinetic potentials,[6] we have not been able to prove this conjecture. If indeed it were true, then by using chords and tangents to the P curves, one could immediately generate a large variety of lower and upper energy *bounds* for the spectra of pure power-law potentials.

Another advantage of using kinetic potentials is that they "almost" mimic the potentials themselves under linear combinations and convex and concave transformations. The kinetic potentials then lead immediately to the spectrum, by means of the Legendre transformation (2.5). For example, if the potential shape is given by

$$f(r)=g^{(1)}(h^{(1)}(r))+g^{(2)}(h^{(2)}(r)) ,$$

then the corresponding kinetic potentials are given approximately by

$$\bar{f}_{nl}(s)=g^{(1)}(\bar{h}^{(1)}_{nl}(s))+g^{(2)}(\bar{h}^{(2)}_{nl}(s)) ,$$

and the approximate spectrum follows in turn from (2.5). We have here an approximate global answer to the very difficult question: How does the spectrum depend on the composition of the potential? In the special case of sums of pure power-law potentials this leads to the general eigenvalue formula (2.19). It then turns out that this general formula is greatly simplified if, instead of the component eigenvalues $E_{nl}(q)$ themselves, one uses their representations $P_{nl}(q)$ and obtains finally the simple formula (5.1). Moreover, these smooth and monotonic P functions are precisely what we have been able to approximate so readily.

ACKNOWLEDGMENTS

Partial financial support of this work by the Natural Sciences and Engineering Research Council of Canada under Grant No. A3438 is gratefully acknowledged.

---

[1] E. Prugovečki, *Quantum Mechanics in Hilbert Space* (Academic, New York, 1981).

[2] M. Reed and B. Simon, *Methods of Modern Mathematical Physics IV: Analysis of Operators* (Academic, New York, 1981).

[3] W. Thirring, *A Course in Mathematical Physics 3: Quantum Mechanics of Atoms and Molecules* (Springer, New York, 1981).

[4] S. Flügge, *Practical Quantum Mechanics* (Springer, New York, 1974); the linear potential is discussed on p. 101.

[5] R. L. Hall (unpublished).

[6] R. L. Hall, J. Math. Phys. **24**, 324 (1983); **25**, 2708 (1984).

[7] R. L. Hall, Phys. Rev. D **30**, 433 (1984).

[8] R. L. Hall, Can. J. Phys. **63**, 311 (1985).